Dominant Hydrometeor Type Distributions within Brazilian Tropical Precipitation Systems Inferred from X-Band Dual Polarization Radar Measurements

Jean-François Ribaud [1], Luiz A.T. Machado [1], and Thiago Biscaro [1]

1 National Institute for Space Research (INPE), Center for Weather Forecast and Climate Studies (CPTEC), Cachoeira Paulista, SP, BRAZIL

1 - Context And Objectives

The present study aims at investigating for the first time the 3D evolution and characteristics of the hydrometeor distributions within brazilian tropical convective systems retrieved by a research polarimetric X-band radar in the frame of CHUVA project. Meteorological events from two Intense Observaton Periods (IOPs), that occurred during both wet and dry seasons respectively, are investigated through radar maesurements that took place in Manaus in 2014 (Amazon region).

Since microphysical description within tropical precipitation systems is pretty rare or even non-existent especially over the Brazil, hydrometeor dominant type distributions are determined by applying a new clustering based algorithm to dual polarization radar measurements. Unlike to the most popular Hydrometeor Classification Algorithms (HCAs) such as fuzzy logic, this clustering approach allows to directly makes the use of the radar measurements without making any first assumptions about polarimetric observable boundaries for each one of potential microphysical species.

This poster focuses on the first results about characteristics of clustering outputs through precipitation events oberseved during both the dry and wet season.

2 – Clustering Approach

The proposed clustering approach is mainly based on Grazioli et al (2015) methodology. It consists in an unsupervised Agglomerative Hierarchical Clustering technique that allows to merge N objects into n clusters (with n < N). Each object is defined by:

$$x = \{Z_H, Z_{DR}, K_{DP}, \rho_{HV}, \Delta z\}$$

where Z_H represents the horizontal reflectivity, Z_{DR} the differential reflectivity, K_{DP} the specific differential phase, ρ_{HV} the coefficient correlation, and Δz the difference between the altitude of the resolution volume considered and the altitude of the isotherm 0°C. Then all of those components are standardized to vary in a same order of magnitude [0;1].

To distinguish between differents objects within the available database two metrics are defined: i) euclidean distance, and ii) centroid merging rule.

A spatial constraint is also implemented to the data-driven clustering method that relies on the spatial smoothness of the partition in the physical space. This restriction aims to improve the spatial consistency of clustering outputs by checking them four nearest neighbouring objects (Bechini et al. 2014; Grazioli et al. 2015; Besic et al, 2016).

Initially the clustering method deals with a subset of ~20 000 observations randomly chosen over P precipitations events, to both save computationally costs and get a first general behaviour of radar measurements.

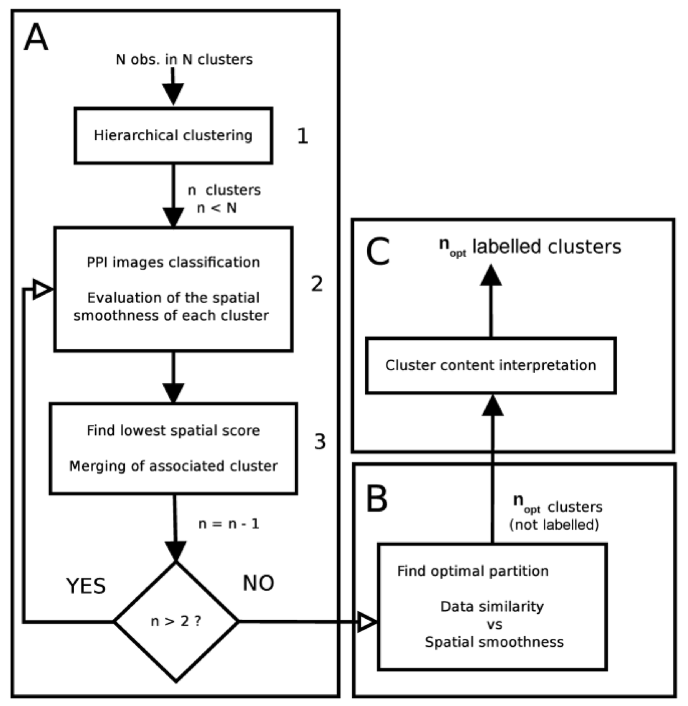

Figure 2.1 Schematic representation of each clustering step – From *Grazioli et al. (2015)*

3 – Cluster qualty metrics

As defined in Grazioli et al. 2015, few independent quality metrics have also been calculated at each iteration of the method to determine the optimal cluster partition between each other:

i) Kappa index: evaluates the global spatial smoothness of the partition. Kappa ranges from -1 to +1 and increases as the level of spatial smoothness increases.

ii) Accuracy Spread index (AS): evaluates the inhomogeneity of the spatial characteristics of a partition into nc clusters in the range [0;1]. Lower values are associated with better partitions.

Optimal partition for the wet season: 6 clusters

Optimal partition for the dry season: 7 clusters

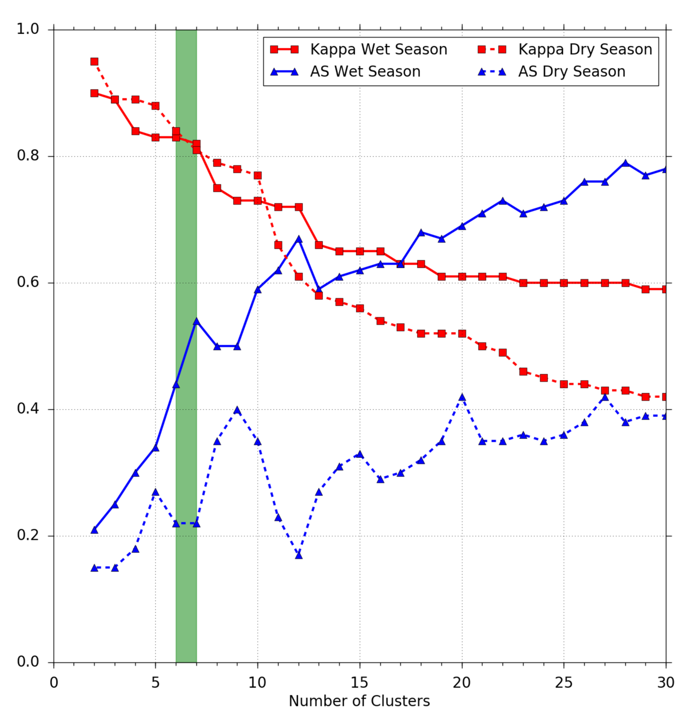

Figure 3.1 Evolution of the cluster quality metrics as a function of the number of clusters.

4 - Results

WET SEASON

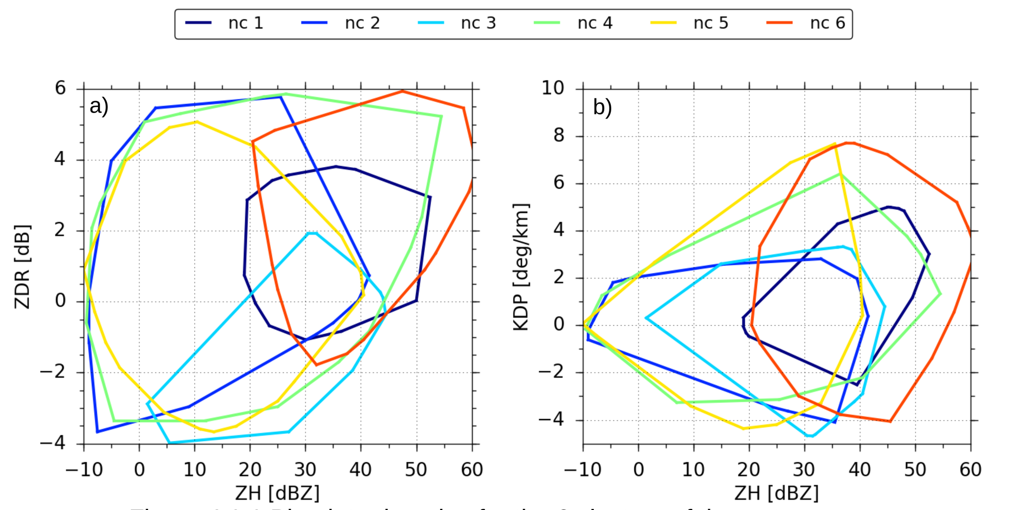

Figure 4.1.1 Bivariate domains for the 6 clusters of the wet season. a) $Z_H - Z_{DR}$, b) $Z_H - K_{DP}$

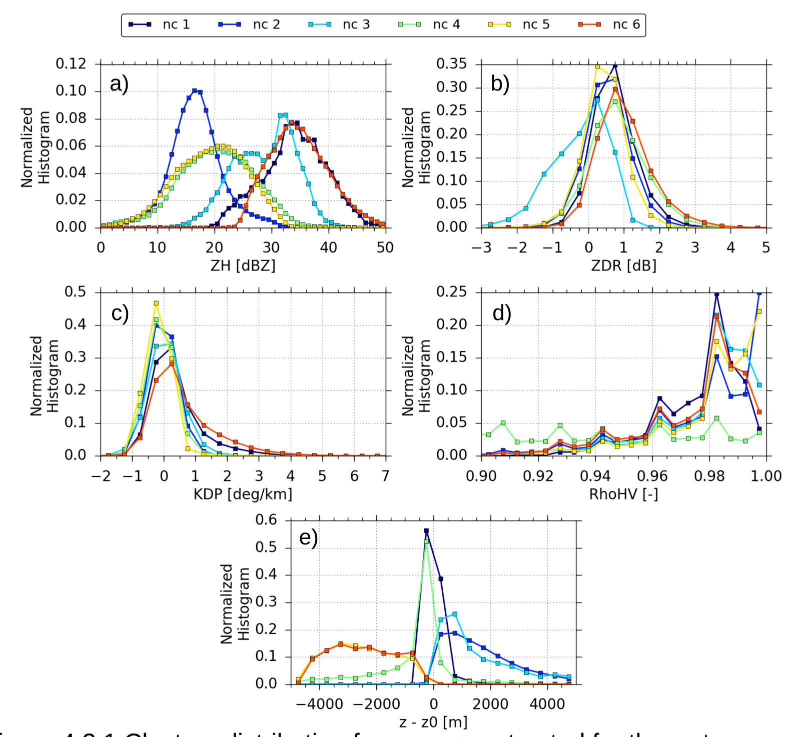

Figure 4.2.1 Clusters distribution for one run extracted for the wet season. a) Z_H [dBZ], b) Z_{DR} [dB], c) K_{DP} [deg/km], d) ρ_{HV} [-], and e) Δz [m].

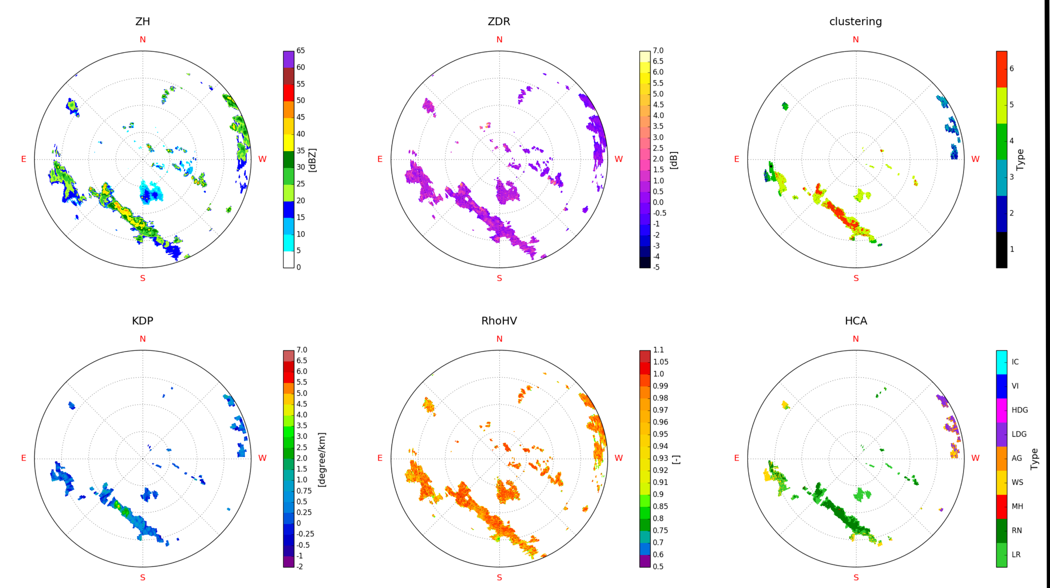

Figure 4.3.1 Polarimetric observation and hydrometeor classification outputs for a PPI scan collected during the GO-AMAZON experiment with an angle of 3.2°. The comparison with the HCA outputs are based on the fuzzy logic of Besic et al, 2016 (adapted from Dolan and Rutledge 2009) with 9 hydrometeor types (LR: Light Rain, RN: Rain, MH: Melting Hail, WS: Wet Snow, AG: Aggregates, LDG: Low Density Graupel, HDG: High Density Graupel, VI: Vertical aligned Ice, and IC: Ice Crystals).

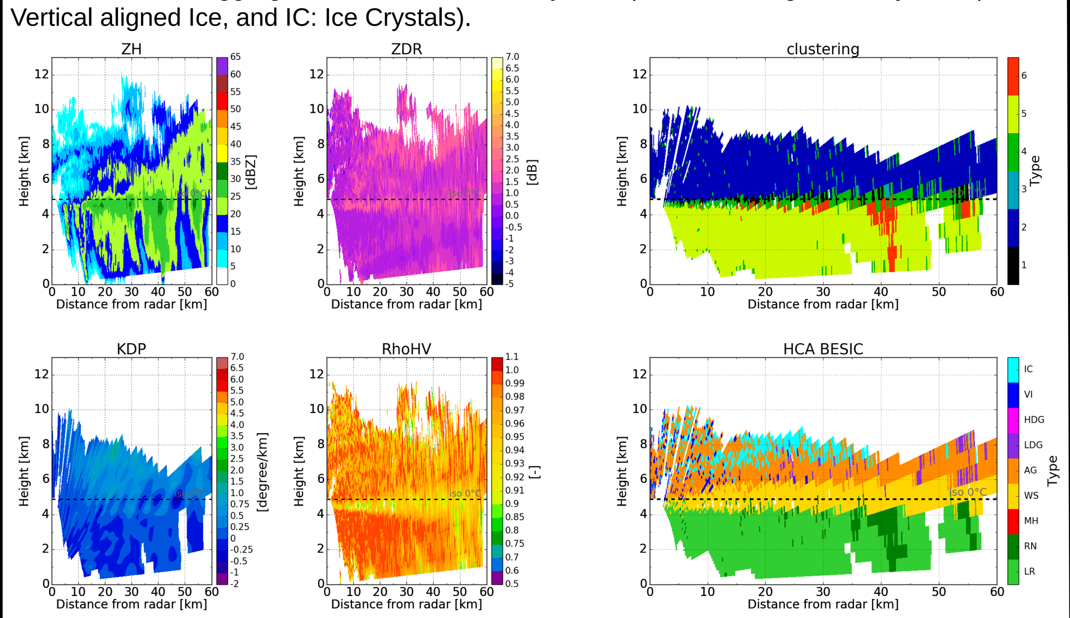

Figure 4.4.1 Polarimetric observation and hydrometeor classification outputs for a RHI scan collected during the GO-AMAZON experiment. The comparison with the HCA outputs are based on the fuzzy logic of Besic et al, 2016 (adapted from Dolan and Rutledge 2009) with 9 hydrometeor types (LR: Light Rain, RN: Rain, MH: Melting Hail, WS: Wet Snow, AG: Aggregates, LDG: Low Density Graupel, HDG: High Density Graupel, VI: Vertical aligned Ice, and IC: Ice Crystals).

DRY SEASON

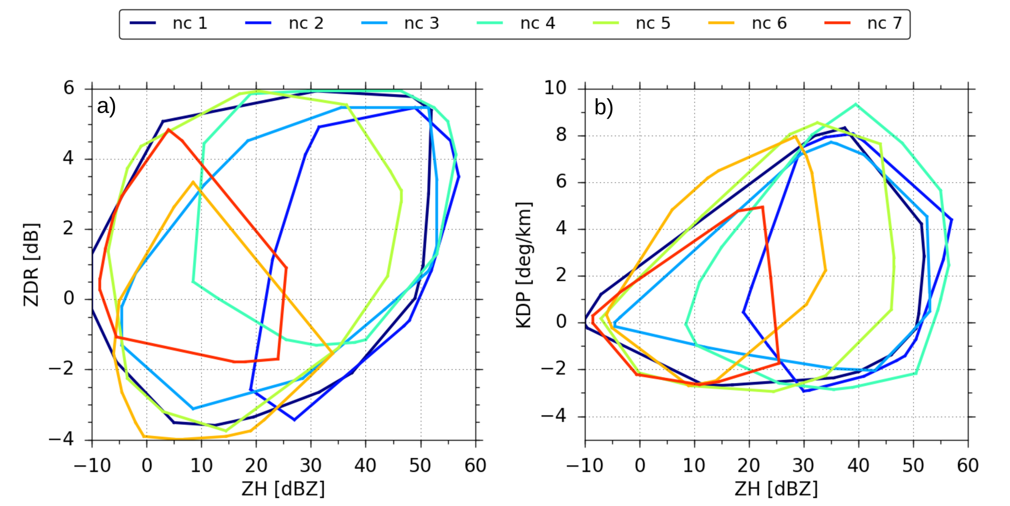

Figure 4.1.2 Bivariate domains for the 6 clusters of the wet season. a) $Z_H - Z_{DR}$, b) $Z_H - K_{DP}$

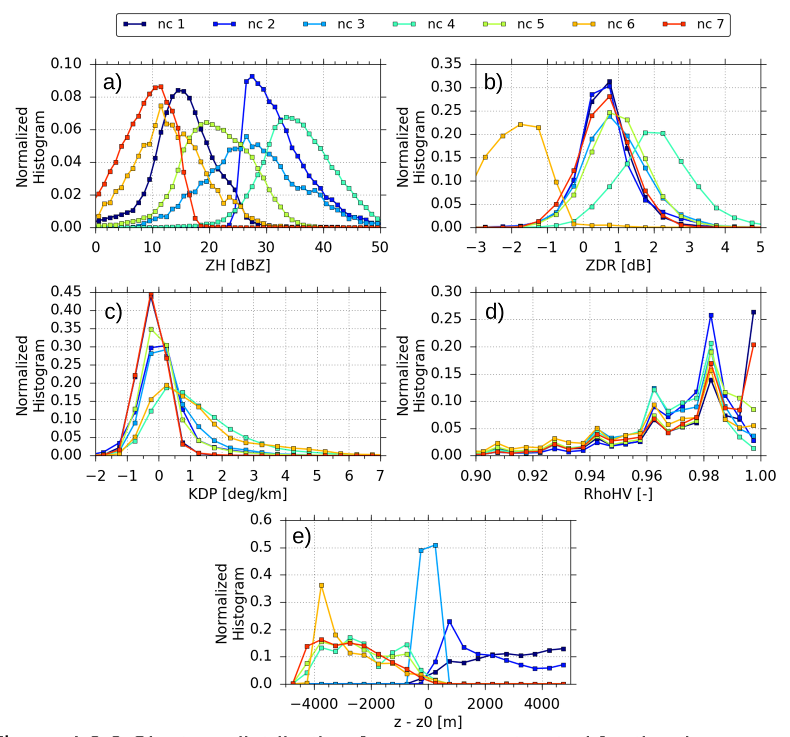

Figure 4.2.2 Clusters distribution for one run extracted for the dry season. a) Z_H [dBZ], b) Z_{DR} [dB], c) K_{DP} [deg/km], d) ρ_{HV} [-], and e) Δz [m].

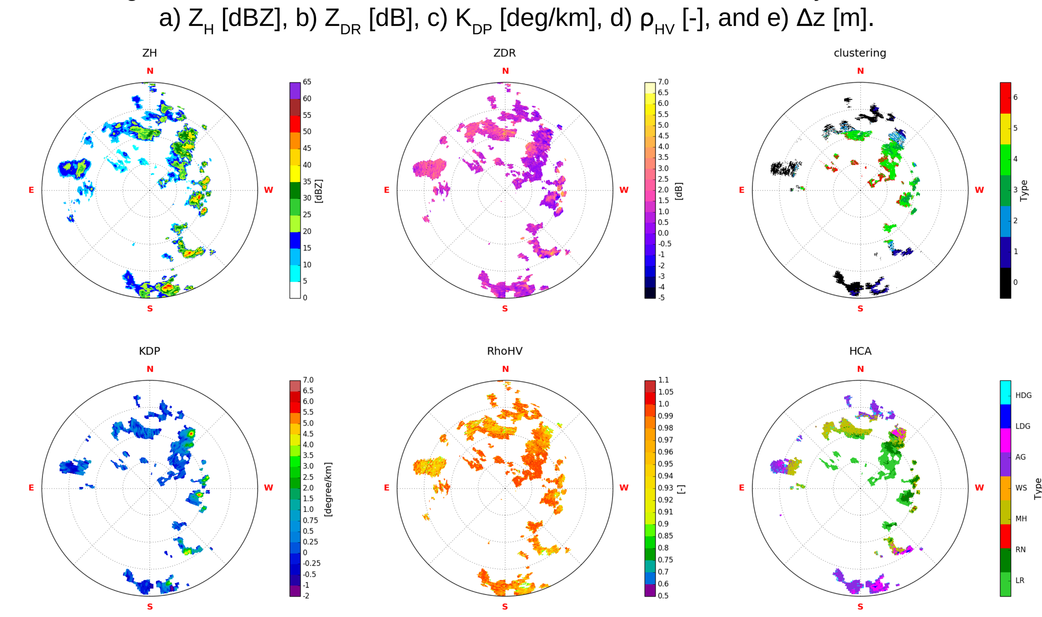

Figure 4.3.2 Polarimetric observation and hydrometeor classification outputs for a PPI scan collected during the GO-AMAZON experiment with an angle of 3.2°. The comparison with the HCA outputs are based on the fuzzy logic of Besic et al, 2016 (adapted from Dolan and Rutledge 2009) with 9 hydrometeor types (LR: Light Rain, RN: Rain, MH: Melting Hail, WS: Wet Snow, AG: Aggregates, LDG: Low Density Graupel, HDG: High Density Graupel, VI: Vertical aligned Ice, and IC: Ice Crystals).

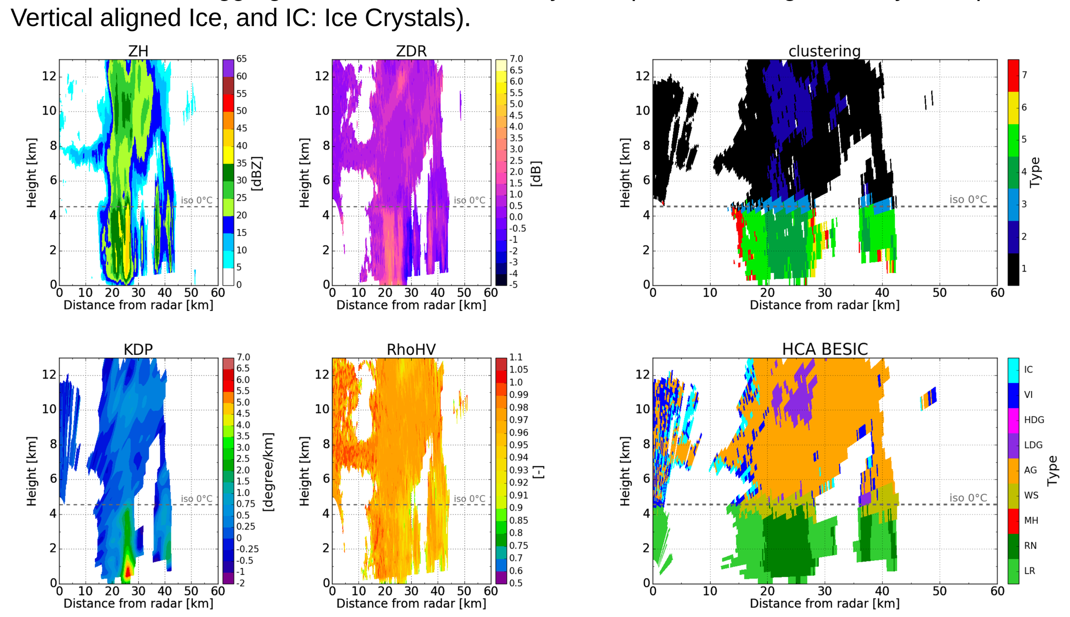

Figure 4.4.2 Polarimetric observation and hydrometeor classification outputs for a RHI scan collected during the GO-AMAZON experiment. The comparison with the HCA outputs are based on the fuzzy logic of Besic et al, 2016 (adapted from Dolan and Rutledge 2009) with 9 hydrometeor types (LR: Light Rain, RN: Rain, MH: Melting Hail, WS: Wet Snow, AG: Aggregates, LDG: Low Density Graupel, HDG: High Density Graupel, VI: Vertical aligned Ice, and IC: Ice Crystals).

5 – Cluster comparisons and DPOL characteristics

WET SEASON

Table 5.1 Confusion matrix comparing each cluster to the fuzzy logic method outputs used in Besic et al, 2016.

TYPE	DZ	RN	MH	WS	DS	LDG	HDG	VI	CR
nc 1	96.96	0.82	0.01	2.09	0.0	0.11	0.01	0.0	0.0
nc 2	0.18	0.01	0.0	16.01	69.21	1.85	0.0	8.76	3.97
nc 3	0.0	0.0	0.0	16.31	25.59	55.13	0.67	2.3	0.01
nc 4	30.24	12.39	0.01	51.5	3.77	0.3	0.0	0.83	0.96
nc 5	82.48	13.42	0.0	4.1	0.0	0.0	0.0	0.0	0.0
nc 6	1.34	91.38	2.01	5.27	0.0	0.0	0.0	0.0	0.0

Table 5.2 Dual polarization characteristics for each different cluster and each different radar observable using the mean value, standard deviation (STD), and set of quantiles (Q).

# Nc	Var	Mean	STD	Q1%	Q5%	Q10%	Q25%	Q50%	Q75%	Q90%	Q95%	Q99%
nc 1	ZH	33.78	5.57	21.5	24.0	26.0	30.0	34.0	37.5	41.0	42.5	45.5
nc 1	ZDR	0.98	0.55	-0.2	0.19	0.35	0.58	0.9	1.29	1.69	1.92	2.63
nc 1	KDP	0.61	0.76	-0.42	-0.14	-0.04	0.13	0.4	0.84	1.59	2.2	3.44
nc 1	RhoHV	0.98	0.01	0.93	0.94	0.96	0.97	0.98	0.99	0.99	0.99	1.0
nc 2	ZH	16.48	4.79	4.0	9.0	11.0	13.5	16.5	19.0	22.5	25.0	29.5
nc 2	ZDR	0.8	0.56	-0.52	-0.05	0.11	0.43	0.82	1.13	1.53	1.76	2.31
nc 2	KDP	0.23	0.35	-0.52	-0.26	-0.16	0.01	0.19	0.41	0.68	0.87	1.23
nc 2	RhoHV	0.98	0.02	0.9	0.93	0.94	0.96	0.98	0.99	1.0	1.0	1.0
nc 3	ZH	28.53	5.45	16.0	19.0	21.0	24.5	29.0	32.5	35.0	36.5	39.0
nc 3	ZDR	-0.01	0.76	-2.17	-1.39	-1.07	-0.52	0.19	0.58	0.82	0.98	1.21
nc 3	KDP	0.29	0.54	-0.91	-0.47	-0.25	0.01	0.27	0.55	0.89	1.15	1.69
nc 3	RhoHV	0.98	0.02	0.91	0.94	0.95	0.97	0.98	0.99	1.0	1.0	1.0
nc 4	ZH	19.99	6.87	1.5	8.5	11.5	15.5	20.0	25.0	28.5	30.5	34.5
nc 4	ZDR	1.05	0.79	-0.83	-0.13	0.19	0.58	0.98	1.53	2.08	2.39	3.26
nc 4	KDP	0.17	0.39	-0.66	-0.35	-0.23	-0.05	0.14	0.35	0.6	0.79	1.4
nc 4	RhoHV	0.92	0.05	0.81	0.83	0.85	0.88	0.92	0.96	0.98	0.99	1.0
nc 5	ZH	18.96	6.21	4.0	8.5	11.0	14.5	19.5	23.5	27.0	28.5	31.0
nc 5	ZDR	0.68	0.53	-0.83	-0.13	0.11	0.43	0.66	0.98	1.29	1.53	2.0
nc 5	KDP	0.08	0.32	-0.51	-0.27	-0.18	-0.06	0.05	0.18	0.35	0.51	1.23
nc 5	RhoHV	0.98	0.02	0.92	0.94	0.95	0.97	0.99	0.99	1.0	1.0	1.0
nc 6	ZH	34.74	5.37	25.0	26.5	28.0	31.0	34.5	38.0	42.0	44.5	49.5
nc 6	ZDR	1.26	0.72	-0.13	0.27	0.5	0.82	1.13	1.61	2.16	2.63	3.5
nc 6	KDP	0.86	1.02	-0.6	-0.17	-0.03	0.18	0.54	1.29	2.25	2.89	4.27
nc 6	RhoHV	0.97	0.02	0.91	0.93	0.94	0.96	0.98	0.99	0.99	1.0	1.0

DRY SEASON

Table 5.3 Confusion matrix comparing each cluster to the fuzzy logic method outputs used in Besic et al, 2016.

TYPE	DZ	RN	MH	WS	DS	LDG	HDG	VI	CR
nc 1	53.61	0.01	0.0	2.06	34.94	1.45	0.02	6.75	1.16
nc 2	0.02	0.0	0.05	10.26	34.5	51.5	3.67	0.0	0.0
nc 3	5.7	11.68	1.3	65.43	1.42	11.83	0.3	2.35	0.0
nc 4	1.7	87.0	2.78	8.08	0.0	0.41	0.02	0.01	0.0
nc 5	64.93	27.82	0.0	7.2	0.0	0.0	0.0	0.03	0.01
nc 6	85.37	8.7	0.0	5.0	0.12	0.16	0.0	0.62	0.04
nc 7	98.47	0.0	0.0	1.24	0.03	0.04	0.0	0.19	0.03

Table 5.4 Dual polarization characteristics for each different cluster and each different radar observable with: the mean value, standard deviation (STD), and set of quantiles (Q).

# Nc	Var	Mean	STD	Q1%	Q5%	Q10%	Q25%	Q50%	Q75%	Q90%	Q95%	Q99%
nc 1	ZH	15.25	5.59	-0.5	6.0	9.0	12.0	15.0	18.5	22.0	24.0	27.5
nc 1	ZDR	0.89	0.69	-0.91	-0.13	0.11	0.5	0.9	1.21	1.69	2.0	2.87
nc 1	KDP	0.05	0.37	-0.83	-0.48	-0.33	-0.14	0.04	0.22	0.44	0.61	1.13
nc 1	RhoHV	0.97	0.03	0.87	0.91	0.93	0.96	0.98	1.0	1.0	1.0	1.0
nc 2	ZH	31.93	5.27	24.5	25.5	26.0	28.0	31.0	35.0	39.5	42.5	47.5
nc 2	ZDR	0.91	0.79	-0.99	-0.2	0.19	0.5	0.82	1.21	1.84	2.47	3.42
nc 2	KDP	0.41	0.85	-1.16	-0.67	-0.37	-0.01	0.28	0.66	1.22	2.01	3.7
nc 2	RhoHV	0.97	0.02	0.88	0.93	0.95	0.96	0.98	0.98	0.99	0.99	1.0
nc 3	ZH	27.46	8.23	9.5	14.5	17.0	22.0	27.0	32.5	38.5	41.5	48.0
nc 3	ZDR	1.16	0.88	-0.83	-0.2	0.19	0.58	1.13	1.69	2.24	2.71	3.57
nc 3	KDP	0.62	0.91	-0.74	-0.31	-0.15	0.07	0.37	0.94	1.71	2.38	3.9
nc 3	RhoHV	0.97	0.02	0.88	0.93	0.94	0.96	0.97	0.98	0.99	0.99	1.0
nc 4	ZH	35.36	6.13	20.5	25.5	28.0	31.5	35.0	39.5	43.5	46.0	49.5
nc 4	ZDR	2.29	1.0	0.03	0.74	1.06	1.61	2.24	2.87	3.57	4.05	4.83
nc 4	KDP	1.39	1.34	-0.85	-0.2	0.04	0.46	1.1	2.05	3.16	3.96	5.77
nc 4	RhoHV	0.97	0.02	0.87	0.92	0.93	0.96	0.97	0.98	0.99	0.99	1.0
nc 5	ZH	20.99	6.14	4.5	11.0	13.5	17.0	21.0	25.5	29.0	30.5	34.0
nc 5	ZDR	1.23	0.81	-0.68	-0.05	0.27	0.74	1.21	1.69	2.24	2.55	3.42
nc 5	KDP	0.39	0.8	-0.88	-0.38	-0.22	-0.01	0.2	0.54	1.2	1.88	3.65
nc 5	RhoHV	0.97	0.03	0.86	0.9	0.92	0.96	0.98	0.99	0.99	1.0	1.0
nc 6	ZH	12.69	6.36	-2.0	2.0	4.5	8.5	12.5	17.0	21.0	24.0	27.5
nc 6	ZDR	-1.69	0.8	-3.51	-3.04	-2.8	-2.25	-1.62	-1.07	-0.83	-0.68	0.66
nc 6	KDP	1.39	1.47	-0.52	-0.17	-0.01	0.31	1.03	1.92	3.58	4.6	5.96
nc 6	RhoHV	0.96	0.03	0.86	0.89	0.91	0.94	0.97	0.98	0.99	1.0	1.0
nc 7	ZH	8.53	4.58	-3.0	0.0	2.0	5.5	9.0	12.0	14.0	15.0	16.5
nc 7	ZDR	0.87	0.69	-0.68	-0.28	-0.05	0.43	0.9	1.29	1.76	2.0	2.55
nc 7	KDP	0.05	0.36	-0.77	-0.43	-0.3	-0.13	0.03	0.2	0.4	0.59	1.23
nc 7	RhoHV	0.97	0.02	0.9	0.93	0.94	0.96	0.98	0.99	1.0	1.0	1.0

6 - Conclusions & Outlook

- The clustering approach technique to classify dominant hydrometeor within radar volumes has been developped for a X-band dual-polarization radar that took place in Amazon region during both wet and dry season in 2014. First results based on radar observable and temperature information show the good consistency of the methodology to detect similar objects.

- The complete cluster content interpretation are actually ongoing through multiple runs. Several aspects are also investigated such as:

→ in-situ measurements (research aircrafts)

→ disdrometers comparisons

→ model outputs (CRSIM)

→ wet / dry season differences for a same hydrometeor class

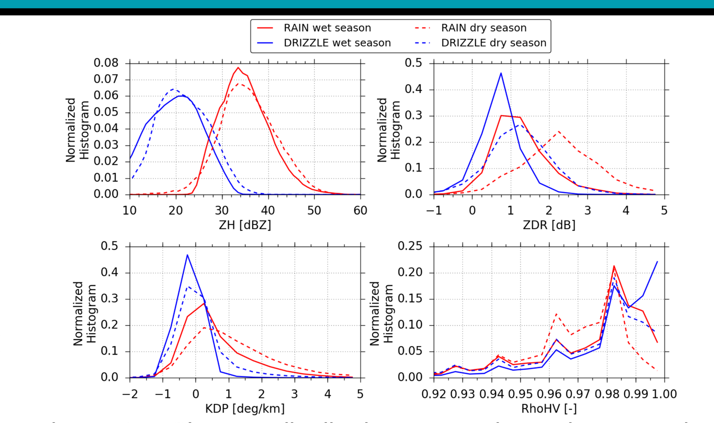

Figure 6.1 Clusters distribution comparisons between the wet and dry seasons for both the rain and drizzle microphysical species. a) Z_H [dBZ], b) Z_{DR} [dB], c) K_{DP} [deg/km], and d) ρ_{HV} [-].

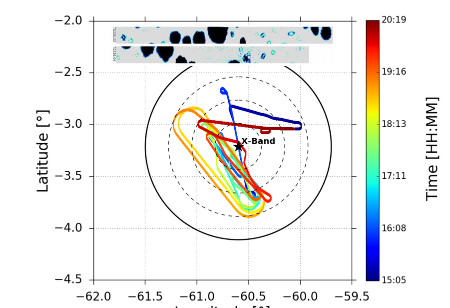

Figure 6.2 HALO airtrack and microphysical observations valid on 09 September 2014.

7 - References

Bechini, R. and Chandrasekar, V.: *A Semisupervised Robust Hydrometeor Classification Method for Dual-Polarization Radar Applications*, J. Atmos. Ocean. Technol., 32, 22–47, 2014.

Besic, N., Grazioli, J., Gabella, M., Germann, U., and Berne, A. *Hydrometeor classification through statistical clustering of polarimetric radar measurements: a semi-supervised approach*. Atmos. Meas. Tech. 9, 2016.

Dolan, B. and Rutledge, S. A.: *A Theory-Based Hydrometeor Identification Algorithm for X-Band Polarimetric Radars*, J. Atmos. Ocean. Technol., 26, 2071–2088, 2009.

Grazioli, J., Tuia, D., and Berne, A.: *Hydrometeor classification from polarimetric radar measurements: a clustering approach*, Atmos. Meas. Tech., 8, 149–170, doi:10.5194/amt-8-149-2015, 2015.

Contact : jean-francois.ribaud@inpe.br

38th Conference on Radar Meteorology, Chicago, IL, USA, 28 august - 1 September 2017